

ORIGINAL RESEARCH PAPER

## Ultrasound assisted electro-Fenton process including Fe-ZSM-5 nanocatalyst for degradation of Phenazopyridine

Mohammad Rostamizadeh<sup>1,2\*</sup>, Soorena Gharibian<sup>1,2</sup>, Samira Rahimi<sup>1,2</sup>

<sup>1</sup> Faculty of Chemical Engineering, Sahand University of Technology, Sahand New Town, Tabriz, Iran.

<sup>2</sup> Research Center of Environmental Engineering, Sahand University of Technology, Sahand New Town, Tabriz, Iran.

Received: 2019-05-07

Accepted: 2019-06-28

Published: 2019-08-01

### ABSTRACT

Pharmaceutical wastewaters have several *negative effects on human health*. This study reports heterogeneous and ultrasound assisted electro Fenton (HSEF) for efficient degradation of Phenazopyridine (PHP). The high silica zeolite socony mobil-5 (ZSM-5) nanocatalyst is synthesized by hydrothermal technique and impregnated with iron species (0.1Fe-ZSM-5). The surface and textural properties of the synthesized nanocatalyst were characterized by X-ray Diffraction (XRD), Transmission electron Microscopy (TEM) and N<sub>2</sub> adsorption-desorption techniques. The nanocatalyst includes the high crystallinity (ca. 72.41 %), surface area (ca. 294.40 m<sup>2</sup>g<sup>-1</sup>) and uniform dispersion of Fe species. The optimum operating conditions of the HSEF system are pH= 7, applied current of 100 mA, 0.1Fe-ZSM-5 nanocatalyst concentration of 0.2 gL<sup>-1</sup> and ultrasonic power of 600 WL<sup>-1</sup> which result in the highest PHP removal efficiency. The high performance of the developed nanocatalyst in three consecutive runs confirms the reusability of the nanocatalyst. The results show that the HSEF system has a high capacity for the efficient removal of PHP without requiring long reaction time, high applied current and strict acidic conditions which candidates it for the industrial applications.

**Keywords:** *Electro Fenton; Heterogeneous; Phenazopyridine; Ultrasound; Zeolite nanocatalyst*

### How to cite this article

Rostamizadeh M, Gharibian S, Rahimi S. Ultrasound assisted electro-Fenton process including Fe-ZSM-5 nanocatalyst for degradation of Phenazopyridine. J. Water Environ. Nanotechnol., 2019; 4(3): 227-235. DOI: 10.22090/jwent.2019.03.005

## INTRODUCTION

Today, industries are known as the main source of water contamination. Pharmaceutical industry introduces synthetic pharmaceuticals into surface and ground waters which are hazardous due to their toxicity and resistivity to biodegradation [1]. Phenazopyridine hydrochloride (PHP) as an analgesic drug is prescribed for pain relieving related to urinary tract infection or irritation [2]. Several research reported the negative effects of PHP on human health such as carcinogenicity in mice, red urine discoloration, headache, hemolytic anemia and methemoglobinemia [2-5]. In order to PHP removal, research to develop a more efficient wastewater treatment is in demand. The common

purification systems are unable to fully remove or degrade persistent molecules including complex azo structures [6; 7]. Advanced Oxidation Processes (AOPs) are mainly based on generation of hydroxyl radicals ( $OH^\cdot$ ,  $E_0 = 2.76V$  [8]) which have been subjected to great interest for wastewater treatment [9]. Among AOPs, Fenton reaction is common due to the low cost and high ability of  $OH^\cdot$  generation [10]. The main restrictions of Fenton process are strict acidic pH control, rapid consumption of  $Fe^{2+}$  rather generation and formation of ferric hydroxide sludge [11]. These restriction are addressed through immobilization of  $Fe^{2+}$  (active phase) onto porous structures (such as zeolite), which improves the feasibility of the heterogeneous Fenton reaction [11].

\* Corresponding Author Email: [Rostamizadeh@sut.ac.ir](mailto:Rostamizadeh@sut.ac.ir),  
[Rostamizadeh.m@gmail.com](mailto:Rostamizadeh.m@gmail.com)



This work is licensed under the Creative Commons Attribution 4.0 International License.

To view a copy of this license, visit <http://creativecommons.org/licenses/by/4.0/>.

Electro Fenton (EF) is an improved form of Fenton reaction due to **in-situ** electro generation of Fenton's reagents [12]. Furthermore, this system is eco-friendly and cost-effective with small operational footprint [13]. The EF process faces some issues like strict acidic pH control and low oxygen solubility in water which is required for electro generation of  $H_2O_2$  [14]. Recently, a coupling strategy of AOP systems has been proposed to improve efficiency [15]. Several studies have proposed coupling of the EF with irradiation of ultrasound waves [16-18]. This can be explained by the formation of  $OH^\cdot$  through thermal dissociation of water molecules due to cavitation of the ultrasound waves (Eqs.2-6) [11; 19; 20]. Turbulence formation by ultrasound waves also leads to the improved mass transfer between solid-liquid phases [19].



where  $))$  denotes the ultrasonic waves. Oturan et al. [13] studied a hybrid system of homogenous sono electro Fenton including  $Fe^{3+}$  ions as catalyst for degradation of some organic pollutants (4,6-dinitro-o-cresol, 2,4-dichlorophenoxyacetic acid and azobenzene). The proposed system had significant improvement compared with Fenton and EF systems as result of the enhanced mass transfer, synergic generation of  $OH^\cdot$  and pyrolysis of pollutant molecules by cavitation. Babuponnusami et al. [21] compared Fenton, EF, photo electro Fenton and sono electro Fenton systems over homogenous  $Fe^{2+}$  catalyst for degradation of phenol. They concluded that sono electro Fenton system had better performance in compare to EF including complete phenol removal and 67.9% mineralization over 40 min. Martinez et al. [16] studied different systems for azure B dye degradation over homogenous  $Fe^{2+}$  catalyst. Their results showed that efficiency of the systems was in the following order: low-frequency sono electro Fenton > Fenton > sonication. Sahinkaya

[17] reported combination of EF and sonication for degradation of Reactive Black 5 using cast iron anodes as Fe catalyst source. Optimum reaction conditions were: pH= 3, current= 250 mA,  $[H_2O_2] = 800 \text{ mgL}^{-1}$  and electrode distance of 2.5 cm. They concluded that efficiency improvement by applying sonication was negligible due to complex nature of textile wastewater. Hassani et al. [19] studied heterogeneous sono Fenton process using  $Fe_3O_4$  catalyst for degradation of Basic Violet 10. Optimum conditions were pH= 3, [catalyst]= 1.5  $\text{gL}^{-1}$ ,  $[H_2O_2] = 36 \text{ mM}$ , ultrasound power of 450  $\text{wL}^{-1}$  and [BV10]= 30  $\text{mgL}^{-1}$  which resulted in 75.94% removal over 120 min. Ma et al. [18] studied the degradation of Acid Orange 7 in aqueous solution by combination of ultrasound and visible light. They reported that the removal efficiency was increased up to 35% when the ultrasound was applied (1 MHz and 40 W). Melero et al. [22] investigated effect of ultrasound on the degradation of phenolic aqueous solution including different nanocomposite at pH of 3. They found that the degradation rate in the presence of the ultrasound was high because it hindered the agglomeration of the catalyst particles. From operational point of view, the main problem of Fenton and EF is homogeneous  $Fe^{2+}$  catalyst which cannot be easily separated for regeneration and reuse [6] which can be solved through heterogeneous electro Fenton (HEF).

It is worth noting that previous studies have investigated the hybrid system of homogenous electro Fenton with ultrasound and there is no report on combination of HEF with ultrasonic waves. For the first time, we coupled HEF with ultrasound waves to apply heterogeneous sono electro Fenton system (HSEF) for PHP removal. The main objective of the hybrid system was chemical and physical effects of ultrasound waves in favor of more  $OH^\cdot$  generation, better  $Fe^{2+}$  regeneration, and high rate of mass transfer and continuous cleaning of heterogeneous catalyst surfaces. Among the heterogeneous catalysts, ZSM-5 has the appropriate textural properties (high surface area and pore volume) and pore size distribution, which has been attracted more attentions for wastewater treatment. We applied the HSEF system for PHP removal using the synthesized ZSM-5 nanocatalyst including Fe species as active phase. Effect of pH, current, catalyst concentration and ultrasonic power were studied.

## MATERIALS AND METHODS

### Materials

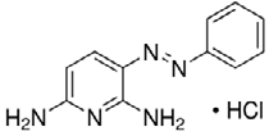
Chemicals for the synthesis of the nanocatalyst were silicic acid ( $\text{SiO}_2 \cdot x\text{H}_2\text{O}$ , > 99 wt.%), sodium aluminate ( $\text{NaAlO}_2$ ,  $\text{Al}_2\text{O}_3$  wt.% = 55), iron nitrate ( $\text{Fe}(\text{NO}_3)_3 \cdot 9\text{H}_2\text{O}$ , 99 wt.%), tetrapropyl ammonium bromide (TPABr,  $\text{C}_{12}\text{H}_{28}\text{BrN}$ , > 99 wt.%), ammonium nitrate ( $\text{NH}_4\text{NO}_3$ , 99 wt.%), sodium hydroxide ( $\text{NaOH}$ , 99.6 wt.%) and sulfuric acid

( $\text{H}_2\text{SO}_4$ , 98 wt.%) which were supplied from Merck (Germany). PHP was kindly donated by Shahre Daru pharmaceutical Company (Iran). General information and specifications of PHP are shown in Table 1.

### Nanocatalyst preparation

The parent nanocatalyst (ZSM-5, Si/Al= 200) was synthesized using hydrothermal method at

Table 1. General information of PHP

Structure	Formula	Molar Mass ( $\text{g}\cdot\text{mol}^{-1}$ )	$\lambda_{\text{max}}$ (nm)
	$\text{C}_{11}\text{H}_{11}\text{N}_5$	213.239	430

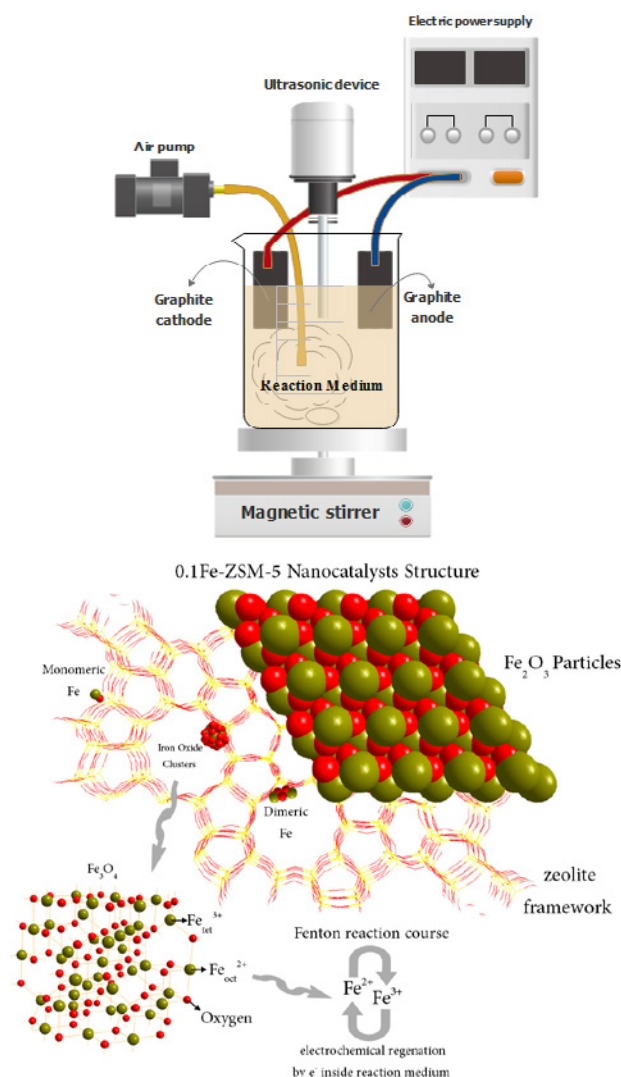


Fig. 1. Schematic of the HSEF bubble reactor and approximate structure of 0.1Fe-ZSM-5.

180 °C and 48 h. The molar composition of the synthesized gel was 20 SiO<sub>2</sub>: 0.05 Al<sub>2</sub>O<sub>3</sub>: 3TPABr: 1.5Na<sub>2</sub>O: 200H<sub>2</sub>O. Wet impregnation of the parent nanocatalyst (HZSM-5) resulted in the bimetallic nanocatalyst including 0.1 wt.% iron promoter (0.1Fe-ZSM-5). N<sub>2</sub> adsorption-desorption, TEM and XRD techniques were used characterized the synthesized nanocatalysts. The detailed procedure for the synthesis and characterization of the nanocatalysts can be found in literature [23].

#### HSEF process

Fig. 1 shows schematic of the HSEF set-up and approximate 0.1Fe-ZSM-5 nanocatalyst structure. Reaction medium included 50 mL of wastewater (10 mgL<sup>-1</sup> of PHP), 0.05 M of Na<sub>2</sub>SO<sub>4</sub> as electrolyte and the nanocatalyst (0.2, 0.6 and 1 g L<sup>-1</sup> of 0.1Fe-ZSM-5). pH level of solution was adjusted by 0.1 M HCl or 0.01 M NaOH solution. The electrodes (graphite, 3 × 2 × 0.5 cm) at the edge of the 100 mL beaker provided electrical current using a DC power supply. Ambient air injection supplied the required oxygen. In each batch, the reaction medium was firstly saturated by O<sub>2</sub> for 5 min. Then, the electrical current was set between the electrodes and simultaneously low frequency (~20 kHz) ultrasound device (Bandelin HD 3000 Series,

Germany) was turned on to generate ultrasound waves inside the reaction medium. Samples were taken at designated times and PHP concentration was determined using spectrophotometric method by UV-vis spectrophotometer (Jinan Hanon instrument Co. Ltd, China) at 430 nm. Removal efficiency was calculated using Eq.6 [24]:

$$\%PHP \text{ removal} = \frac{C_0 - C_t}{C_0} \times 100 \quad (6)$$

where C<sub>0</sub> and C<sub>t</sub> are PHP concentration in initial wastewater and sample, respectively.

## RESULTS AND DISCUSSION

### Nanocatalyst characterization

The nanocatalysts include MFI-structure of ZSM-5 in consistent with standard ZSM-5 (JCP: 00-044-0002) (Fig. 2). The relative crystallinity is the ratio of the peak area located at 2θ= 22.5-24.5° in compare with the parent nanocatalyst (ZSM-5). 0.1Fe-ZSM-5 nanocatalyst has the lower relative crystallinity (Table 2) which is in agreement with an amorphous peak located at 2θ= 25.5-27°. This can be explained by dealumination through the impregnation process which leads to slight framework defects and shifted peak positions (Fig. 2). It is reported that the framework destruction

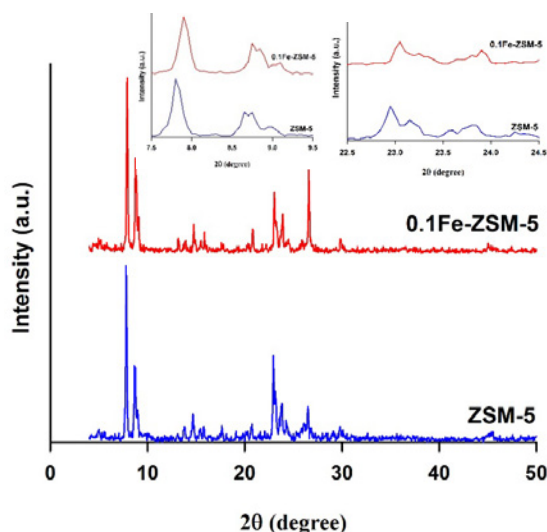


Fig. 2. The XRD patterns of the nanocatalysts (Inside patterns are the zoom in the range of 2θ=7.5-9.5 and b) 2θ=22.5-24.5).

Table 2. Relative crystallinity and textural data (BET surface area, total volume of pores, microporous volume and mesoporous volume) of the nanocatalysts

Sample	Crystallinity (%)	S <sub>BET</sub> (m <sup>2</sup> g <sup>-1</sup> )	V <sub>total</sub> (cm <sup>3</sup> g <sup>-1</sup> )	V <sub>micro</sub> (cm <sup>3</sup> g <sup>-1</sup> )	V <sub>meso</sub> (cm <sup>3</sup> g <sup>-1</sup> )
ZSM-5	100.00	321.10	0.19	0.13	0.06
0.1Fe-ZSM-5	72.41	294.40	0.17	0.11	0.06

through dealumination shifted peak position to the high  $2\theta$  values [25]. TEM images of the HZSM-5 and 0.1Fe-ZSM-5 nanocatalysts are shown in Fig. 3. It is clear that the aggregation of the nanocrystals forms the microspheres which is in consistent with literature [23; 26].

$N_2$  adsorption-desorption of the nanocatalysts are a combination of isotherm types I and IV (Fig. 4a). The rectangular type H4 hysteresis loops at the high relative pressure ( $P/P_0 = 0.5-0.95$ ) is assigned to the mesoporous structure based on the capillary condensation [27]. The mesoporous structure is created by the crystal agglomeration in the form of interparticle space. The high adsorption volume at the very low relative pressure ( $P/P_0 = 0.1$ ) is attributed to the microporous structures [28]. The pore size distribution of the nanocatalysts confirms the formation of mesoporous structure (Fig. 4b). The major pore diameter of the nanocatalysts is 1.70 nm. The calculated textural data show the high surface area and total pore volume (Table 2). The low BET surface area and pore volume of the bimetallic nanocatalyst results from the slightly

damage or blockage of the pores. The results agree with the XRD results.

Acidimetric-alkalimetric titration [29] of the ZSM-5 and 0.1Fe-ZSM-5 nanocatalyst determines  $pH_{pzc}$  equal to 3.6 and 4, respectively. In fact, the introduction of Fe species through the impregnation hides some acid sites from accessible surface [30]. The surface hydroxyl groups (OH) attain positive charge at  $pH < pH_{pzc}$  and negative charge at  $pH > pH_{pzc}$  which influences adsorption capacity of the nanocatalyst at different pH levels.

#### Effect of operational parameters on HSEF efficiency pH level

It is accepted that pH is the most important operational parameter in the field of AOPs especially Fenton [31; 32]. pH directly influences characteristics of both pollutant and catalyst including solubility, surface charges and ionization. It is reported that PHP has abnormal solubility over the wide range of pH [33]. Therefore, determination of the optimum pH level for the proposed HSEF system is important. Fig. 5 shows PHP removal

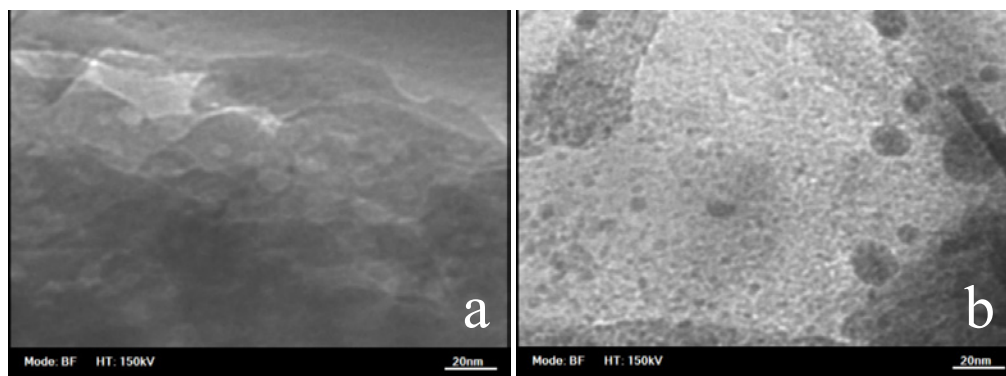


Fig. 3. TEM image of the a) HZSM-5 and b) 0.1Fe-ZSM-5 nanocatalysts.

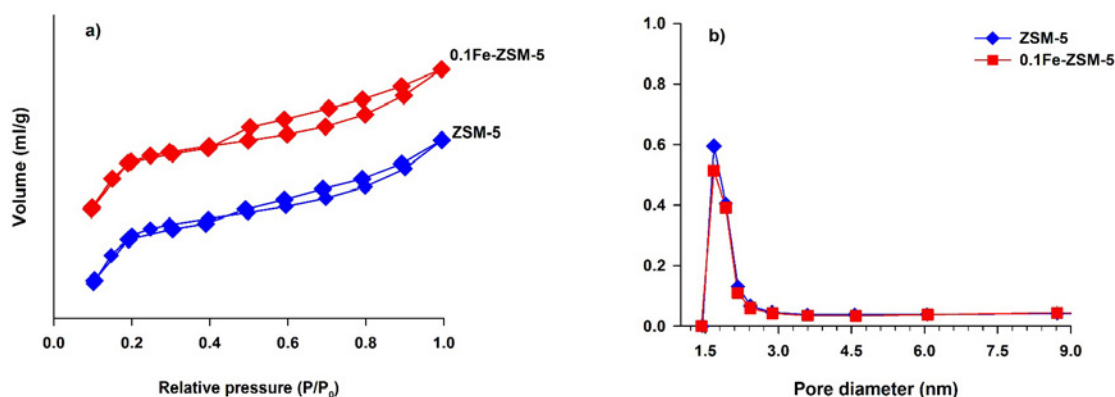
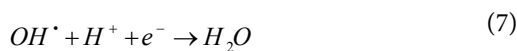


Fig. 4. a)  $N_2$  adsorption-desorption isotherm and b) pore size distribution of the nanocatalysts

efficiency as function of pH. At pH= 3, the HSEF system has 74% removal efficiency after 30 min of the reaction. By increasing pH to 5, PHP removal efficiency decreases to 60% due to lower oxidation ability of  $OH^\cdot$ , ferric hydroxide formation scavenging effect of  $OH^\cdot$  by  $H^+$  (Eq.7), unstable nature and decomposition of  $H_2O_2$  (Eq.8) [6].

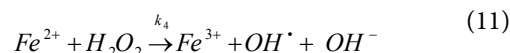
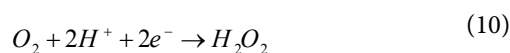
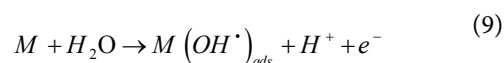


PHP removal efficiency is increased at pH of 7. This phenomenon can be explained by electrostatic interactions due to surface charges of the nanocatalyst and ionization state of PHP. At pH levels higher than  $pH_{pzc}$  of 0.1Fe-ZSM-5 nanocatalyst (4), surface hydroxyl groups generate negative charges around the particles [34]. On the other hand, PHP is a basic drug and attains positive form at pH levels higher than its  $pka$  (5.15) [33]. Therefore, electrostatic interaction between the nanocatalyst particles and PHP molecules results in more adsorption [35]. Further increase in pH level toward alkaline conditions has insignificant improvement of PHP removal owing to unstable nature of  $H_2O_2$  in alkaline conditions and less oxidation ability of  $OH^\cdot$  radical [31]. It is concluded that the HSEF system has considerable removal ability at neutral pH level which leads to less operational complicity and cost. Hence, pH= 7 is selected as the optimum pH level and further tests are conducted at this pH level.

#### Effect of current

The applied current between anode and cathode leads to *in-situ* generation of Fenton reagents

(Eqs.10-12) and anodic oxidation (Eq.9) which is considered a direct cost of the HSEF system [13].



Therefore, optimization of current as an operational parameter is very important for the system optimization. Effect of current on PHP removal is studied at four levels of 0, 100, 200 and 300 mA (Fig. 6). In order to determine adsorption contribution through PHP removal in the HSEF system, adsorption test is conducted at optimum pH= 7, 0.2  $gL^{-1}$  of 0.1Fe-ZSM-5 nanocatalyst and without current between electrodes (0 mA) which results in 51% PHP removal. PHP molecules are adsorbed by cage like structure (Fig. 1) of 0.1Fe-ZSM-5 nanocatalyst through Van Der Waals, hydrophilic, hydrogen bonding or electrostatic interactions [34]. The current between electrodes (100 mA) improves PHP removal up to 90%. It is concluded that PHP removal by the HSEF system is attributed to both adsorption and oxidation mechanism [36]. The higher current (200 mA) increases amount of the available electrons for regeneration of  $Fe^{2+}$  in the reaction medium (Eq.12) and also more  $H_2O_2$  are produced (Eq.10) which leads to generation of more  $OH^\cdot$  on active sites of 0.1Fe-ZSM-5 nanocatalyst. However, the very high current (300 mA) saturates active sites

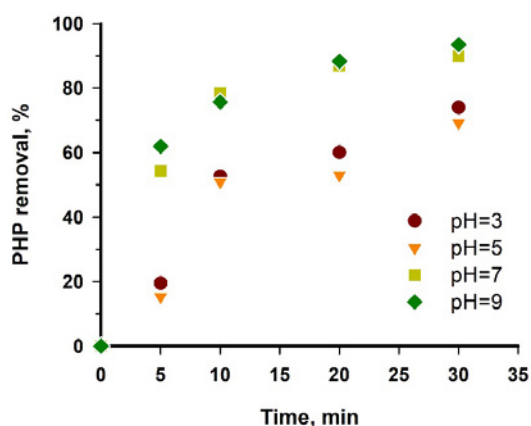


Fig. 5. PHP removal efficiency of the HSEF at different pH levels. Reaction conditions: 0.1Fe-ZSM-5 concentration of 0.2  $gL^{-1}$ , applied current of 100 mA, ultrasonic power of 600  $WL^{-1}$ .

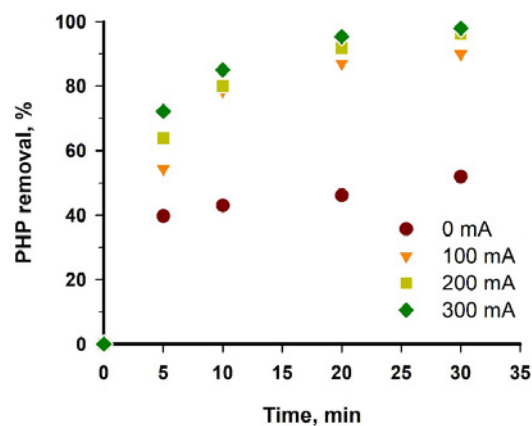
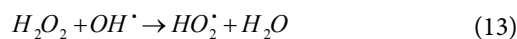


Fig. 6. PHP removal efficiency of the HSEF at different applied currents. Reaction conditions: pH=7, 0.1Fe-ZSM-5 concentration of 0.2  $gL^{-1}$ , ultrasonic power of 600  $WL^{-1}$ .

and excessive amounts of  $H_2O_2$  act as scavenger for  $OH^\cdot$  radicals (Eq.13) [37].



Based on structural and mechanical properties of graphite electrodes, the higher currents ( $> 200mA$ ) accelerate destruction of the sacrificial graphite anode in return for insignificant PHP removal improvement. From economical and operational point of view, the rapid destruction and frequent replacement of the anode is unfavorable. Therefore, 100 mA is considered as optimum level of current and further tests are conducted at this level.

#### Catalyst concentration

It is reported that concentration of catalyst plays a key role in efficiency of Fenton based reactions [19]. Also, amount of required catalyst should be optimized due to economic considerations. Therefore, effect of catalyst concentration in the HSEF system is studied at 3 levels (Fig. 7). 0.2  $gL^{-1}$  concentration of 0.1Fe-ZSM-5 nanocatalyst shows 90% PHP removal efficiency in the HSEF system. Increasing of the catalyst concentration (0.6  $gL^{-1}$ ) reduces removal efficiency. Hassani et al. [19] studied sono Fenton system for basic violet 10 removal. Their results showed that high  $Fe^{2+}$  concentration improved removal efficiency up to a certain point (76%) and then decreased as result of scavenging effect of  $Fe^{2+}$  catalyst towards  $OH^\cdot$  (Eq.14).

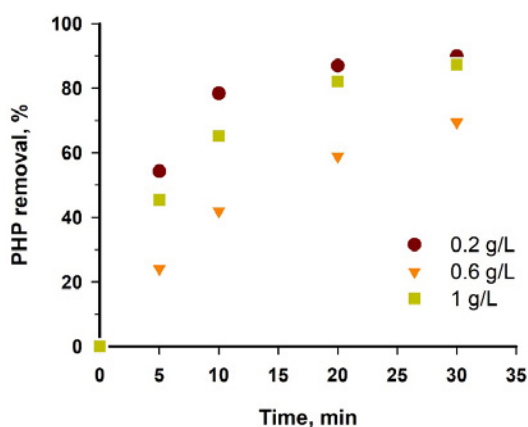


Fig. 7. PHP removal efficiency of the HSEF using different amount of 0.1Fe-ZSM-5 nanocatalyst. Reaction conditions: pH=7, applied current of 100mA, ultrasonic power of 600  $WL^{-1}$ .

In the HSEF system, increasing of the catalyst concentration from 0.6 to 1  $gL^{-1}$  enhances PHP removal from 69 to 87%, respectively. This can be explained by the increasing of the adsorption at the high catalyst concentration which overcomes the scavenging effect of excessive  $Fe^{2+}$  sites. But this negative effect cannot be neglected as PHP removal at 1  $gL^{-1}$  which is still lower than 0.2  $gL^{-1}$ . Hence, the catalyst concentration of 0.2  $gL^{-1}$  is an optimum for the HSEF system.

#### Ultrasound power

As discussed in Section 3.2, the ultrasonic waves facilitate mass transport and  $OH^\cdot$  production which suppress the electro Fenton limitations and draw backs [11]. But, utilization of the ultrasound waves requires energy and must be optimized as an operational parameter. Effect of the ultrasonic power in PHP removal is studied at 3 levels of 600, 1000 and 2000  $WL^{-1}$  (Fig. 8). Increasing of ultrasound power decreases PHP removal significantly. It is proposed that higher ultrasonic powers lead to degassing of reaction solution which results in the less  $OH^\cdot$  generation due to shortage of  $O_2$  in the solution (Eqs. 10-12) [13]. However, the HSEF system including the low ultrasound power (600  $WL^{-1}$ ) has the higher efficiency in compare to the HEF system at the same operational conditions. Therefore, the ultrasound power equal to 600  $WL^{-1}$  is an optimum level.

#### Reusability

One of the main advantages of the heterogeneous catalysts is the easy and low cost recovering of the spent catalyst for the further applications in AOPs

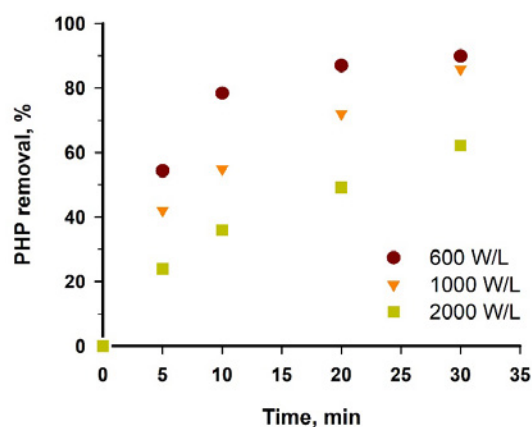


Fig. 8. PHP removal efficiency of the HSEF at different ultrasonic power. Reaction conditions: pH=7, 0.1Fe-ZSM-5 concentration of 0.2  $gL^{-1}$ , applied current of 100 mA.

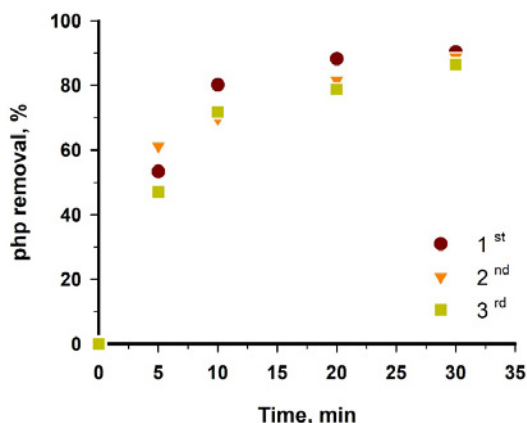


Fig. 9. Reusability of 0.1Fe-ZSM-5 nanocatalyst for PHP removal. Reaction conditions: pH=7, applied current of 100 mA, ultrasonic power of 600 WL<sup>-1</sup>.

[11]. However, heterogeneous Fenton catalysts may lose catalytic activity due to different phenomena including iron leaching, pore blocking as a result of pollutant adsorption and change in nature of iron species (such as Fe(OH)O formation) [38]. After each run, the nanocatalyst was recovered from the final effluent by centrifugation. The regeneration of the nanocatalyst was at 55 °C for 6 h (3 °Cmin<sup>-1</sup>) to remove the adsorbed organic species from the nanocatalyst active sites. In order to evaluate stability and reusability of the regenerated 0.1Fe-ZSM-5 nanocatalyst, three consecutive HSEF cycles were carried out at the optimum operational conditions: pH=7, applied current of 100 mA, 0.1Fe-ZSM-5 nanocatalyst concentration of 0.2 gL<sup>-1</sup> and ultrasound power of 600 WL<sup>-1</sup> (Fig. 9). The results confirm that 0.1Fe-ZSM-5 nanocatalyst show insignificant reduction of the catalytic activity for PHP removal (ca. 5%) after 3 consecutive HSEF cycle. The stability of the synthesized 0.1Fe-ZSM-5 nanocatalyst depends on different factors including the effect of ultrasound waves on cleaning of the surface and pores [22], the enhanced exit of PHP molecules and oxidized intermediates from pores due to the high surface area and total pore volume [24] and the calcination of the formed Fe(OH)O during the oxidation process. The slight decrease in PHP removal may be attributed to formation of the larger iron oxide particles. These results prove the high potential of the HSEF system using the reusable 0.1Fe-ZSM-5 nanocatalyst.

## CONCLUSION

In this study, the hybrid HSEF system was applied for the efficient removal of PHP using

the synthesized 0.1Fe-ZSM-5 nanocatalyst. Characterization of the nanocatalyst showed the high crystallinity, high surface area and well dispersion of Fe species in the structure of the bimetallic nanocatalyst. The HSEF system successfully addressed the potential limitations and drawbacks of the homogeneous electro Fenton system owing to the physicochemical effects of the ultrasound waves including mass transfer improvement and the high rate of OH<sup>•</sup> production. The optimum operational conditions were obtained as pH= 7, applied current of 100 mA, 0.1Fe-ZSM-5 nanocatalyst concentration of 0.2 gL<sup>-1</sup> and ultrasonic power of 600 WL<sup>-1</sup>. The developed nanocatalyst showed the high capacity of reusability which had less than 5% loss of the removal efficiency after three consecutive cycles. Consequently, the HSEF system using 0.1Fe-ZSM-5 nanocatalyst has the high potential for the efficient PHP removal from pharmaceutical wastewater including the less reaction time and energy consumption.

## CONFLICTS OF INTEREST

There are no conflicts to declare.

## REFERENCES

- Divyapriya G, Srinivasan R, Nambi IM, Senthilnathan J. Highly active and stable ferrocene functionalized graphene encapsulated carbon felt array - A novel rotating disc electrode for electro-Fenton oxidation of pharmaceutical compounds. *Electrochimica Acta*. 2018;283:858-70.
- Shargh M, Behnajady MA. A high-efficient batch-recirculated photoreactor packed with immobilized TiO<sub>2</sub>-P25 nanoparticles onto glass beads for photocatalytic degradation of phenazopyridine as a pharmaceutical contaminant: artificial neural network modeling. *Water Science and Technology*. 2016;73(11):2804-14.
- Fathinia M, Khataee A, Aber S, Naseri A. Development of kinetic models for photocatalytic ozonation of phenazopyridine on TiO<sub>2</sub> nanoparticles thin film in a mixed semi-batch photoreactor. *Applied Catalysis B: Environmental*. 2016;184:270-84.
- Mahdizadeh F, Aber S, Karimi A. Synthesis of nano zinc oxide on granular porous scoria: Application for photocatalytic removal of pharmaceutical and textile pollutants from synthetic and real wastewaters. *Journal of the Taiwan Institute of Chemical Engineers*. 2015;49:212-9.
- Zyoud AH, Zaatar N, Saadeddin I, Ali C, Park D, Campet G, et al. CdS-sensitized TiO<sub>2</sub> in phenazopyridine photo-degradation: Catalyst efficiency, stability and feasibility assessment. *Journal of Hazardous Materials*. 2010;173(1-3):318-25.
- Nidheesh PV, Olvera-Vargas H, Oturan N, Oturan MA. Heterogeneous Electro-Fenton Process: Principles and Applications. *The Handbook of Environmental Chemistry*: Springer Singapore; 2017. p. 85-110.
- Jafarizad A, Rostamizadeh M, Zarei M, Gharibian S.



- Mitoxantrone removal by electrochemical method: A comparison of homogenous and heterogeneous catalytic reactions. *Environmental Health Engineering and Management*. 2017;4(4):185-93.
8. Dang HT, Le TK. Precursor chain length dependence of polymeric precursor method for the preparation of magnetic Fenton-like CuFe<sub>2</sub>O<sub>4</sub>-based catalysts. *Journal of Sol-Gel Science and Technology*. 2016;80(1):160-7.
  9. Vosoughi M, Fatehifar E, Derafshi S, Rostamizadeh M. High efficient treatment of the petrochemical phenolic effluent using spent catalyst: Experimental and optimization. *Journal of Environmental Chemical Engineering*. 2017;5(2):2024-31.
  10. Khataee A, Vahid B, Aghdasinia H, Bagheri R. Semi-pilot scale fluidized bed reactor for removal of a textile dye through heterogeneous Fenton process using natural pyrite. *International Journal of Environmental Science and Technology*. 2017;15(2):289-300.
  11. Poza-Nogueiras V, Rosales E, Pazos M, Sanromán MÁ. Current advances and trends in electro-Fenton process using heterogeneous catalysts – A review. *Chemosphere*. 2018;201:399-416.
  12. Garcia-Rodriguez O, Lee YY, Olvera-Vargas H, Deng F, Wang Z, Lefebvre O. Mineralization of electronic wastewater by electro-Fenton with an enhanced graphene-based gas diffusion cathode. *Electrochimica Acta*. 2018;276:12-20.
  13. Oturan MA, Sirés I, Oturan N, Pérocheau S, Laborde J-L, Trévin S. Sono-electro-Fenton process: A novel hybrid technique for the destruction of organic pollutants in water. *Journal of Electroanalytical Chemistry*. 2008;624(1-2):329-32.
  14. Ngo TPH, Le TK. Polyethylene glycol-assisted sol-gel synthesis of magnetic CoFe<sub>2</sub>O<sub>4</sub> powder as photo-Fenton catalysts in the presence of oxalic acid. *Journal of Sol-Gel Science and Technology*. 2018;88(1):211-9.
  15. González-García J, Esclapez MD, Bonete P, Hernández YV, Garretón LG, Sáez V. Current topics on sono-electrochemistry. *Ultrasonics*. 2010;50(2):318-22.
  16. Martínez SS, Uribe EV. Enhanced sonochemical degradation of azure B dye by the electro-Fenton process. *Ultrasonics Sonochemistry*. 2012;19(1):174-8.
  17. Şahinkaya S. COD and color removal from synthetic textile wastewater by ultrasound assisted electro-Fenton oxidation process. *Journal of Industrial and Engineering Chemistry*. 2013;19(2):601-5.
  18. Ma CY, Xu JY, Liu XJ. Decomposition of an azo dye in aqueous solution by combination of ultrasound and visible light. *Ultrasonics*. 2006;44:e375-e8.
  19. Hassani A, Karaca C, Karaca S, Khataee A, Açışlı Ö, Yılmaz B. Enhanced removal of basic violet 10 by heterogeneous sono-Fenton process using magnetite nanoparticles. *Ultrasonics Sonochemistry*. 2018;42:390-402.
  20. Li H, Rostamizadeh M, Mameri K, Boffito DC, Saadatkah N, Rigamonti MG, et al. Ultrasound assisted wet stirred media mill of high concentration LiFePO<sub>4</sub> and catalysts. *The Canadian Journal of Chemical Engineering*. 2018;97(8):2242-50.
  21. Babuponnusami A, Muthukumar K. Advanced oxidation of phenol: A comparison between Fenton, electro-Fenton, sono-electro-Fenton and photo-electro-Fenton processes. *Chemical Engineering Journal*. 2012;183:1-9.
  22. Melero JA, Martínez F, Molina R. Effect of Ultrasound on the Properties of Heterogeneous Catalysts for Sono-Fenton Oxidation Processes. *Journal of Advanced Oxidation Technologies*. 2008;11(1).
  23. Rostamizadeh M, Yaripour F, Hazrati H. Ni-doped high silica HZSM-5 zeolite (Si/Al = 200) nanocatalyst for the selective production of olefins from methanol. *Journal of Analytical and Applied Pyrolysis*. 2018;132:1-10.
  24. Rostamizadeh M, Jafarizad A, Gharibian S. High efficient decolorization of Reactive Red 120 azo dye over reusable Fe-ZSM-5 nanocatalyst in electro-Fenton reaction. *Separation and Purification Technology*. 2018;192:340-7.
  25. Rebrov EV, Seijger GBF, Calis HPA, de Croon MHJM, van den Bleek CM, Schouten JC. The preparation of highly ordered single layer ZSM-5 coating on prefabricated stainless steel microchannels. *Applied Catalysis A: General*. 2001;206(1):125-43.
  26. Chen L, Zhu SY, Wang YM, He M-Y. One-step synthesis of hierarchical pentasil zeolite microspheres using diamine with linear carbon chain as single template. *New Journal of Chemistry*. 2010;34(10):2328.
  27. Rostamizadeh M, Taeb A. Synthesis and Characterization of HZSM-5 Catalyst for Methanol to Propylene (MTP) Reaction. *Synthesis and Reactivity in Inorganic, Metal-Organic, and Nano-Metal Chemistry*. 2015;46(5):665-71.
  28. Darabi Mahboub MJ, Rostamizadeh M, Dubois J-I, Patience GS. Partial oxidation of 2-methyl-1,3-propanediol to methacrylic acid: experimental and neural network modeling. *RSC Advances*. 2016;6(115):114123-34.
  29. Kragović M, Daković A, Sekulić Ž, Trgo M, Ugrina M, Perić J, et al. Removal of lead from aqueous solutions by using the natural and Fe(III)-modified zeolite. *Applied Surface Science*. 2012;258(8):3667-73.
  30. Rostamizadeh, M., Jalali, H., Naeimzadeh, F., & Gharibian, S. 2019. Efficient Removal of Diclofenac from Pharmaceutical Wastewater Using Impregnated Zeolite Catalyst in Heterogeneous Fenton Process. *Physical Chemistry Research*, 7, 37-52.
  31. Brillas E, Sirés I, Oturan MA. Electro-Fenton Process and Related Electrochemical Technologies Based on Fenton's Reaction Chemistry. *Chemical Reviews*. 2009;109(12):6570-631.
  32. Ince NH, Tezcanli-Güyer G. Impacts of pH and molecular structure on ultrasonic degradation of azo dyes. *Ultrasonics*. 2004;42(1-9):591-6.
  33. Avdeef, A., Voloboy, D., & Foreman, A. 2007. Dissolution and Solubility A2 - Taylor, John B. In D. J. Trigg (Ed.). *Comprehensive Medicinal Chemistry II* (pp. 399-423). Oxford: Elsevier.
  34. Valdés H, Tardón RF, Zaror CA. Role of surface hydroxyl groups of acid-treated natural zeolite on the heterogeneous catalytic ozonation of methylene blue contaminated waters. *Chemical Engineering Journal*. 2012;211-212:388-95.
  35. Brião GV, Jahn SL, Foletto EL, Dotto GL. Adsorption of crystal violet dye onto a mesoporous ZSM-5 zeolite synthesized using chitin as template. *Journal of Colloid and Interface Science*. 2017;508:313-22.
  36. Kušić H, Koprivanac N, Selanec I. Fe-exchanged zeolite as the effective heterogeneous Fenton-type catalyst for the organic pollutant minimization: UV irradiation assistance. *Chemosphere*. 2006;65(1):65-73.
  37. Liu H, Li XZ, Leng YJ, Wang C. Kinetic modeling of electro-Fenton reaction in aqueous solution. *Water Research*. 2007;41(5):1161-7.
  38. Queirós S, Morais V, Rodrigues CSD, Maldonado-Hódar FJ, Madeira LM. Heterogeneous Fenton's oxidation using Fe/ZSM-5 as catalyst in a continuous stirred tank reactor. *Separation and Purification Technology*. 2015;141:235-45.